Multi-chamber tyre designing for fuel economy

Aldhufairi, Hamad; Olatunbosun, Oluremi; Essa, Khamis

Document Version
Peer reviewed version

Multi-Chamber Tyre Designing for Fuel Economy

Hamad Sarhan Aldhufairi[1], Oluremi Ayotunde Olatunbosun[1] and Khamis Essa[1]

[1] University of Birmingham, Department of Mechanical Engineering, Birmingham, B15 2TT, UK

Abstract:

Rolling-resistance plays a major role in tyre development due to its significant influence on energy consumption and environmental impact. Numerous efforts to minimise the tyre's rolling-resistance have met with no or minor success because of the tyre's complexity and the involved compromises. This paper explores a novel design solution of multi-chamber tyre, as a potential alternative, for low rolling-resistance while meeting other driving requirements; a multi-purpose generalised solution (design-for-all). A novel multi-chamber design (base design) with a validated finite-element (FE) model was used to create the different novel designs. Statistical analysis based on Design of Experiment (DOE) was conducted to identify the best cavity volumes and inflation settings. The "design-for-all" solution offered a 28% reduction in rolling-resistance, an enhanced cornering performance, a matching grip and a satisfactory cushioning.

Keywords:

1. Introduction

To maintain mobility, the vehicle can spend up to 30% of its fuel to overcome the tyres' rolling-resistance depending on its driving cycle.[1] Based on that, the rolling-resistance can have a considerable influence on the vehicle's emissions, its energy sustainability and hence environmental impact, especially on the global scale. This makes addressing the rolling-resistance one of the core requirements in tyre development.[2, 3] Nevertheless, the attempt to lower the rolling-resistance is a difficult task to achieve without compromising other tyre properties because of the tyre's structural complexity. Further insights on this are explored in a previous study.[1]

As a promising substitute, the multi-chamber tyre solution has the likelihood to decrease rolling-resistance without undermining other tyre properties undesirably.[4] In this field, some multi-chamber tyre solutions have been suggested as untested and patented design ideas. The majority of those solutions are for supporting run-flat rolling, securing the tyre beads' position and/or preserving inflation-air.[5-9] Generally, those solutions consist of multiple, self-sustained and annular chambers that are laid adjacently or concentrically to compensate for any failed chambers during operation. For better off-roadway grip, further patented designs were proposed in either concentric circular compartments or removable circular shoe-casing for the tyre's tread.[10-12] Yet, those patents have doubtful validity, practicability, and ability to achieve of the vehicle's various driving needs because they target only a specific need without any solid verification given.

Lambe[13] and Merz et al.[14], each suggested a patented design that may reduce energy losses and ride discomfort via utilizing concentric circular twin-chambers where the inside compartment is set at inferior pressure to that of the outside. With no validations, such design is questionable because it can undermine the tyre's grip, beads mounting stability, and rolling steadiness.

For tyre manufacturers, each of Bridgestone[15] and Goodyear[16] proposed a prospective design idea of multi-chamber tyre for better rolling performance under diverse driving situations by manipulating the tyre's outer-shape and its stiffness via altering compartments' pressures individually and variously. However, those designs are currently under on-going research and yet to be finalised as end products. Coyote[17] produced an interior compartment for the standard tyre turning it into concentric double compartments where the inside cavity has a higher pressure for holding the beads firmly in place and supporting run-flat operation while the lower pressure outside cavity provides for better off-road grip.

Fusion Innovation[18] had an uncompleted project where Kubba[19] studied a four compartments tyre prototype empirically and showed that the multiple cavities solution can decrease the rolling-resistance. In this study, Kubba built an FE tyre model through Abaqus/Standard which was restricted to computing the quasi-static parameters primarily and the lateral forces to some degree but failed to calculate the rolling-resistance and address the interaction between cavity-air and tyre structure.

Overall, the current published research has a shallow coverage of the field of multi-chamber tyre especially in relation to rolling-resistance since it is still an immature research area either in designing phase or laboratory crafting with no real-world uses so far. Furthermore, relevant long-term development projects are under-way by both vehicle and tyre manufacturers but are of restricted access due to commercial confidentiality. Clearly, more detailed and thorough studies are required to be performed both analytically and experimentally. This is to identify the working principles, the various characteristics, and the contribution of the multi-chamber concept to the rolling-resistance and other driving requirements as a prospective alternative solution.

In this regard, this paper uses a novel multi-chamber design, from a previous work[4], as a base design to generate further novel designs in an attempt to reach an optimum multi-chamber design for low rolling-resistance. A multi-purpose (generalised) design is introduced that is tailored for low rolling-resistance while satisfying other essential driving requirements like grip and cushioning (i.e. design-for-all). To identify the optimum design, the generated designs are investigated for the effects of its chambers design, cavity volume, and inflation pressure on the rolling-resistance and other driving requirements compared to the standard tyre design. All the investigations are carried out using Abaqus/Explicit FE and DoE approaches.

2. Study Approach

2.1 Investigation Scope

To independently investigate the structural effects of the multi-chamber designs, the core rolling-resistance due only to the tyre's internal losses (i.e., mechanical hysteresis) is evaluated which is primarily responsible for 80-95% of rolling-resistance compared to other secondary sources like road-slip (i.e., 5%) and aerodynamic-drag (i.e., ~15%) for straight rolling on flat road.[1] In this respect, the targeted tyres are investigated under free-rolling conditions over a smooth surface drum to exclude the contributions of traction, braking and road coarseness to the rolling-resistance. The tyres are contact driven by the road drum and tested once both are in full-contact at steady-state rolling of constant speed to eliminate or minimise any contact slippage to negligible levels. Furthermore, the tyre(s) will be tested at a fixed low rolling-velocity to discount the aerodynamic resistance effect over the tyre's rolling-resistance.

The effect of the anticipated "weight" difference between the different tyre designs is not considered since it is outside this paper's scope. This is because the tyre's rotational inertia has hardly any impact on rolling-resistance during straight free-rolling in which its influence is more perceptible in traction-and-deceleration situations.

Furthermore, "design manufacturability" is another aspect that will not be covered in this paper's scope but in upcoming future works as it requires extensive investigation work and resources of its own. The same goes for the "inflation mechanism" of the tyre.

In this paper, the tyre's rolling-resistance is calculated as the mechanical energy-lost per unit-distance travelled.

2.2 Prototype Designing and Constraints

Several constraints were to be met in creating the novel multi-chamber designs (i.e., II-1 designs) out of the base design (i.e., design II) in Figure 1. First, chamber re-designing is to involve only zones 1 and 2 in the "base design" without including the side zones (L) and (R) to avoid any disruptions to the flexibility of the tyre's main sidewalls. Secondly, the new designs are to have no more than two chambers radially and no more than two chambers laterally. This is in attempt to keep the new designs simple, feasible, and cost-effective. Thirdly, the inflation pressure is to be kept the same between the chambers aligned adjacently in the lateral direction in zones 1 and 2 to have a balanced tyre rolling. Furthermore, zone 1 chambers are to have the highest pressure followed by lower pressure chambers by a minimum difference of 35 KPa consecutively over zone 2 radially as in Figure 2.[17] This is to hold the tyre's beads tightly, support zone 2 chambers, cope with run-flat scenarios, and avoid profile distortions. Lastly, a middle curvy inner-wall was used in zone 2 in some designs to replace the straight inner-wall, to have a more dynamically balanced tyre, have fewer chambers, and avoid a permanently stiffer tyre.

2.3 FE Model Development

This study uses an experimentally validated FE model of an initial multi-chamber design (i.e., design II), from a previous work[4], as a "base design" to produce and evaluate further novel designs (i.e., II-1 designs). In this previous work, as seen in Figure 1, a 225/55 R17 standard tyre was built in Abaqus FE and validated experimentally for rolling-resistance and other driving requirements. Later, this standard tyre was modified to have dual

chambers instead of a single cavity and tested both in FE and experimentally. Using the validated FE model, "design II" was developed and attained after evaluation against different basic multi-chamber designs.
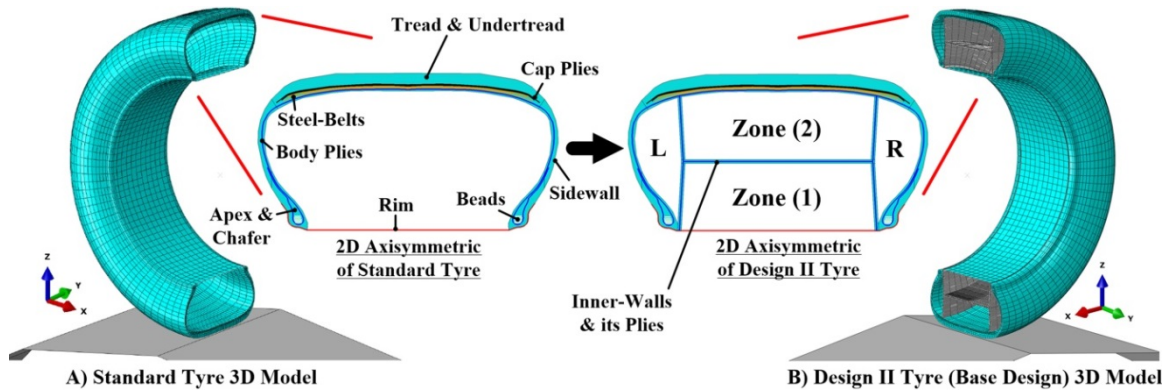
Figure 1. FE Model for Standard and Design II (Base Design) Tyres.

Using full-factorial DoE, as in Figure 2, four novel multi-chamber designs were created including the base design (design II), which was re-numbered to design II-1-1, to assess the effects of different internal chamber designs on the tyre's rolling-resistance. Those novel designs have exactly the same geometrical and material tyre aspects as the "base design" (design II) FE model including the inner-walls for constructing the internal tyre chambers. The only difference is in the number, position and shape of inner-walls.
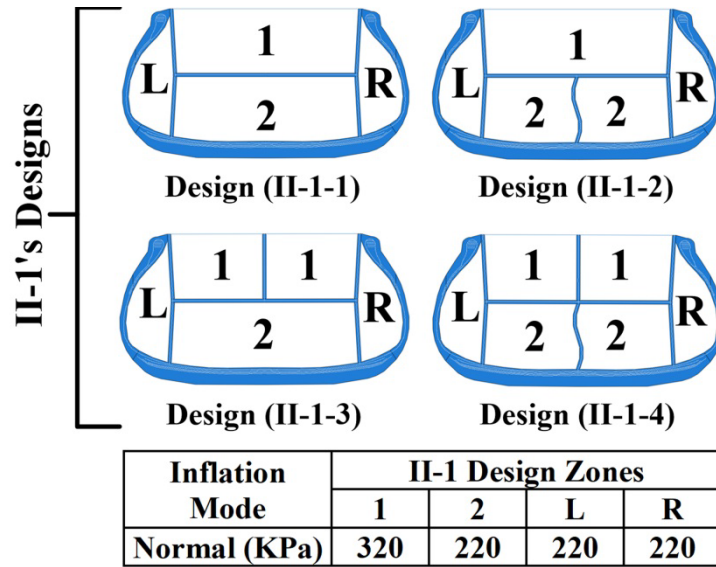
Figure 2. Novel Multi-Chamber II-1 Designs.

Inflation Mode	II-1 Design Zones			
	1	2	L	R
Normal (KPa)	320	220	220	220

Greater details on the FE model development for both the standard and the base (design II) tyres can be found from former investigations.[4, 20] Briefly, full 3D tyre FE models were created using Abaqus 6.13 with analytical rigid road-drum. A groove-free tread was included to minimise hour-glassing and ensure an efficient model as the tread's grooves have marginal influence over tyre's rolling-resistance.[1, 21-23] The tyre's rubber sections were constructed using C3D8R solid elements while the reinforcements were treated as SFM3D4R surface elements embedded within the relevant rubber components. To simulate the physical process of tyre rolling, the related hyperelastic and viscoelastic material properties of the tyre's rubber parts were represented using Yeoh and PRF (Parallel Rheological Framework) modules respectively, while the reinforcements were characterised by its elastic properties, in Abaqus. The insides of the tyre's chambers were considered surface-based fluid-filled cavities using volume elements to represent the inflation air response as an ideal gas.[24-26] Abaqus/Explicit is used for the tyre modelling

to predict the dynamical non-linearity more effectively and because the PRF material model is not compatible with Abaqus/Standard.

2.4 Design Solution

Based on the generated II-1 designs in Figure 2, a multi-purpose generalised design is targeted to meet the diverse driving requirements in which it is customized for low rolling-resistance while maintaining the tyre's grip, cushioning, and cornering stiffness compared to the standard tyre. "Design II-1" set is assessed as it seems to have better manufacturability and offer more versatility to meet the intended application.

Once a sub-optimum design is reached, the effect of the design's cavity volumes on the driving requirements is studied with different cavity volumes within certain limits, as illustrated in Table 2, to maintain design feasibility.

With the optimum volume settings, similarly, the effect of inflation pressure is evaluated within a given working range, as indicated in Table 4, to ensure maintaining tyre profile and operation properly.

2.5 Assessment Conditions

The new multi-chamber designs are evaluated using the validated FE model in Abaqus/Explicit for low rolling-resistance and meeting tyre's gripping, cushioning and cornering performance. The investigation will involve assessing at straight free-rolling the "rolling-resistance" based on the tyre's internal losses (i.e. hysteresis), the "grip"

according to the contact-patch area and the contact-pressure distribution, and the "cushioning" based on the radial static stiffness. At free-rolling under different slip-angles, the "cornering" is assessed in terms of the cornering stiffness and the contact-patch area.

The methodology used in computing the tyre's rolling-resistance, gripping, cushioning and cornering performances can be found in former works[4, 20] for further details. Briefly, in the FE solution, the tyre's rolling-resistance was determined based on the energy dissipated at the tyre's footprint which was obtainable from the product of the FE outputs of the tyre's hysteresis ratio (i.e. ALLCD/ALLIE) against the work done by the tyre at the footprint due to deformation under vertical loading.

The evaluation involves running the tyres at a straight free-rolling velocity of 30 Km/h, under a 4000 N vertical load, and at the normal inflation mode as in Figure 2 unless otherwise stated. The "normal mode" is used whenever the tyre's gripping and cushioning is needed for situations as traction, deceleration, cornering and/or rolling over bumpy roads. For cornering, the tyre(s) runs under the same vertical load at the normal mode but at a free-rolling velocity of 10 Km/h and different slip-angles; at multiple slip-angles that are close to zero for cornering stiffness assessment (i.e., 0, 0.5, 1.0 and 1.5 degrees) and at 3 degrees for footprint area evaluation. The cornering stiffness is calculated from the slope of the cornering force against the slip-angle.

3. Design-for-All

In the "design-for-all", the tyre's "grip" will have priority for safety and driving performance, followed by "cornering" for turns handling and stability, "rolling-resistance" for fuel-economy, and "cushioning" for ride comfort respectively.

3.1 Multi-chamber Design

At the normal mode, the rolling performance of the II-1 designs, shown in Figure 2, is assessed revealing that each design exhibits certain trade-offs with respect to the diverse driving requirements. For the tyre's grip, as seen in Figure 3(a) and Table 1, both the contact-patch area and the contact-pressure distribution of the tyre's footprint are assessed, since they are the core characteristics of the grip mechanism, similar to Aldhufairi et al.[4]. In Table 1, the pressure patterns are used as a generalised estimation of the footprint shape since Abaqus/Explicit does not support a contour visualization of the footprint area. Both designs "II-1-1" and "II-1-3" showed footprint area and shape close to that of the "standard design", whereas designs "II-1-2" and "II-1-4" showed smaller footprints. This is due to the added radial stiffness gained by designs "II-1-2" and "II-1-4"; because of the increase in the numbers of side inner-walls in the designs' zone 2, which noticeably reduced the deformation at the contact-patch.

(a) Footprint Area at Straight Rolling (mm^2).

(b) Cornering Stiffness (N/deg).

(c) Footprint Area (mm^2) at 3 Degrees Slip.

(d) Rolling-Resistance Coefficient.

(e) Radial Static Stiffness (N/mm).
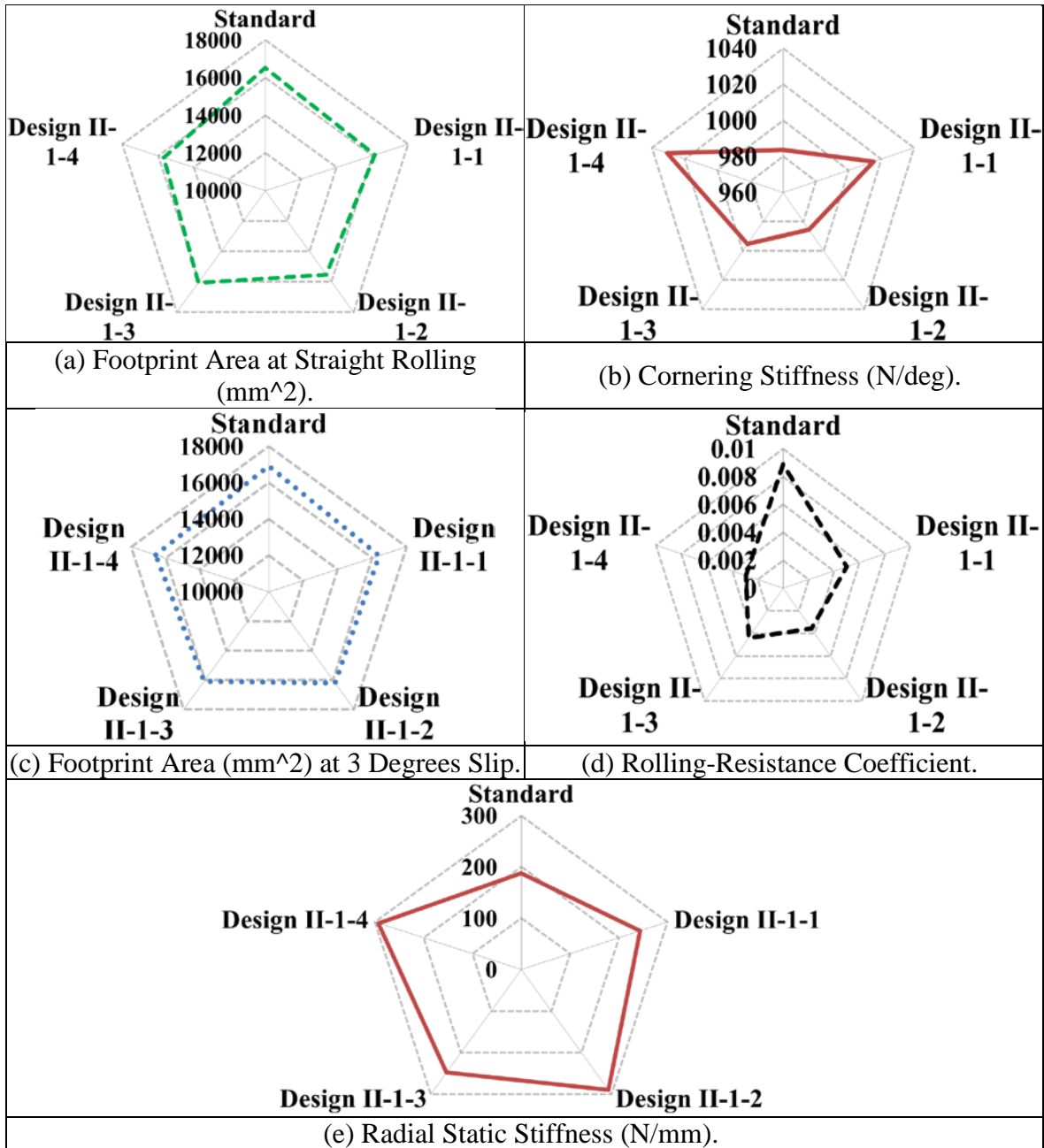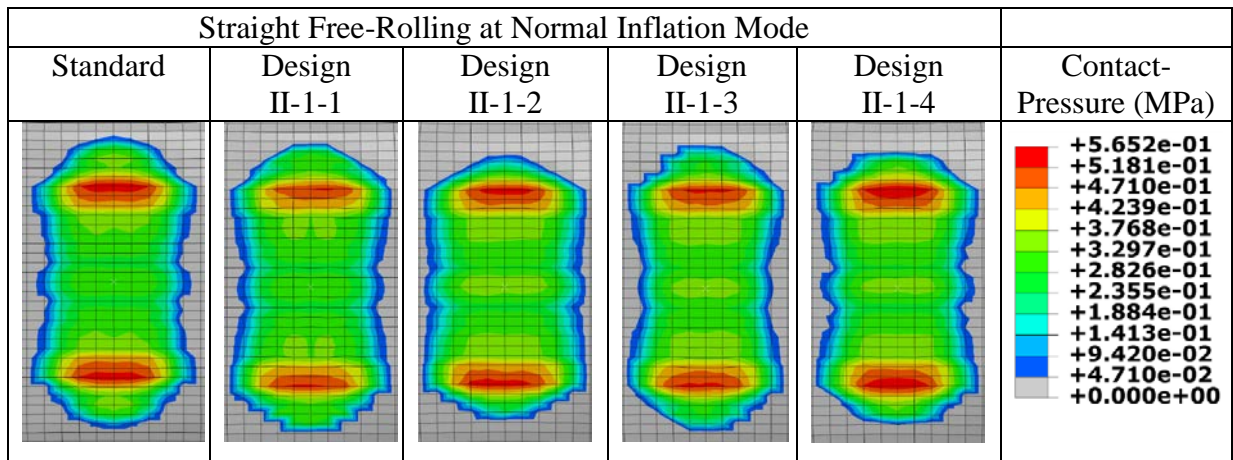
Figure 3. II-1's Designs Performance.

For the contact-pressure, in Table 1, designs "II-1-1" and "II-1-3" exhibited quite different pressure pattern in contrast with the "standard design". The difference can be attributed to the interference of zone 2's side inner-walls with the loading mechanism of the tread region as a result of the inner-walls being a direct rigid-like link of vertical

loading with orthogonal orientation to the tread. Such a difference is minimised with designs "II-1-2" and "II-1-4" due to the middle curvy inner-wall in zone 2 acting more like a spring and a support, with more flexibility and friendly orientation to the tread, reducing the direct loading of the straight zone 2 inner-walls on the tread.

Table 1. Contact-Pressure Pattern for II-1's Designs Footprint.

Straight Free-Rolling at Normal Inflation Mode					
Standard	Design II-1-1	Design II-1-2	Design II-1-3	Design II-1-4	Contact-Pressure (MPa)
					+5.652e-01 +5.181e-01 +4.710e-01 +4.239e-01 +3.768e-01 +3.297e-01 +2.826e-01 +2.355e-01 +1.884e-01 +1.413e-01 +9.420e-02 +4.710e-02 +0.000e+00

In cornering, as illustrated in Figure 3 (b) and (c), II-1 designs demonstrated an increased cornering stiffness to that of "standard design". This is because zone 2's side inner-walls would provide an added support to the tyre's sidewalls laterally during cornering to counteract the relevant opposing centrifugal forces of the vehicle. All II-1 designs displayed smaller footprint area, with a slight difference for designs "II-1-1" and "II-1-4", compared to the standard design.

In II-1 designs, the further confinement of the cavity-air into separate compact spaces, especially in the direct path supporting the tread profile, prevented bulky air-volume losses from the zones supporting the tread directly at the contact-patch during tyre rolling; helping to reduce the tyre's deformation. This is in line with the kinetic theory of

ideal gases and findings of Aldhufairi et al.[4]. Moreover, the utilization of the side inner-walls, especially the straight type, in the multi-chamber construction has provided II-1 designs with an apparent boosted radial stiffness, as shown in Figure 3(e), because it helped in making the vertical loading path more direct to the tread in the tyre's structure agreeing with Ji[27]. This made II-1 designs less prone to structure deformation especially the tread curvature. The more inner-chambers used, particularly in zone 2, the greater the design's radial stiffness would be. In Figure 3(d), such added design stiffness has reduced the rolling-resistance significantly but at the expense of poorer cushioning.

Taken all together, none of the current II-1 designs addresses all the diverse driving requirements satisfactorily. Accordingly, further improvements were made to the most promising design in the current II-1 designs (i.e. design "II-1-1") in an attempt to reach a more fulfilling design to all driving requirements. Compared to the other II-1 designs, design "II-1-1" was picked since it has the closest footprint area to that of the standard design, the lowest rough ride level, and the simplest structure with fewest parts to manufacture.

After several re-designing trials, the modified design "II-1-1B" in Figure 4 was obtained, which involved altering the shape and the orientation of zone 2's side inner-walls from straight rigid-like to curvy spring-like, to gain more flexibility and have more supportive loading path to the tread contact-patch. The overall performance of the design is shown in the next section.
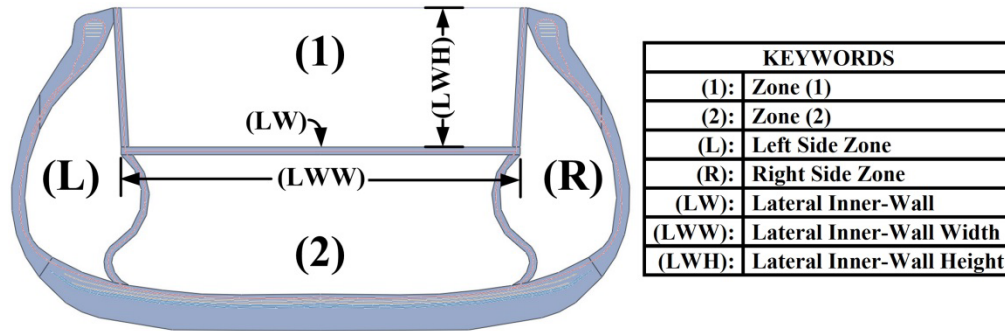
Figure 4. Modified Design (II-1-1B) for "Design-for-All".

3.2 Cavity Volume Effect

Based on full-factorial DoE, twenty-five different versions of design (II-1-1B)'s cavity volumes were created and evaluated for the diverse driving requirements using Abaqus/Explicit. This was done by altering the cross-sectional height and width of the "lateral inner-wall" (LW) in Figure 4 within the dimensional constraints in Table 2.

Table 2. DoE's Factors and their Levels for Cavity Volume Effect.

No	Factor	Dimensional Levels (mm)
1	Lateral Inner-Wall Height (LWH)	30
		38
		45
		53
		60
2	Lateral Inner-Wall Width (LWW)	110
		121
		132
		143
		154

To avoid redundancy and maintain conciseness, samples of the DoE's run results and not all are presented which cover the population's trends and findings as follow:

For the tyre's grip, as shown in Figure 5 (a) and (b) for example, the footprint area was found to increase through either increasing the lateral inner-wall's width at any fixed height above 38 mm or raising the height at the maximum width fixed at 154 mm. Such an effect could be due to the lay-up axes of the side inner-walls of both zones 1 and 2 getting closer to the direct vertical loading path as the lateral inner-wall's width increases. This would mean the vertical loading would be transferred more directly and largely via the side inner-walls to the tread region leading to greater footprint deformation.

| (a) Footprint Area vs Inner-wall's Width. | (b) Footprint Area vs Inner-wall's Height. |

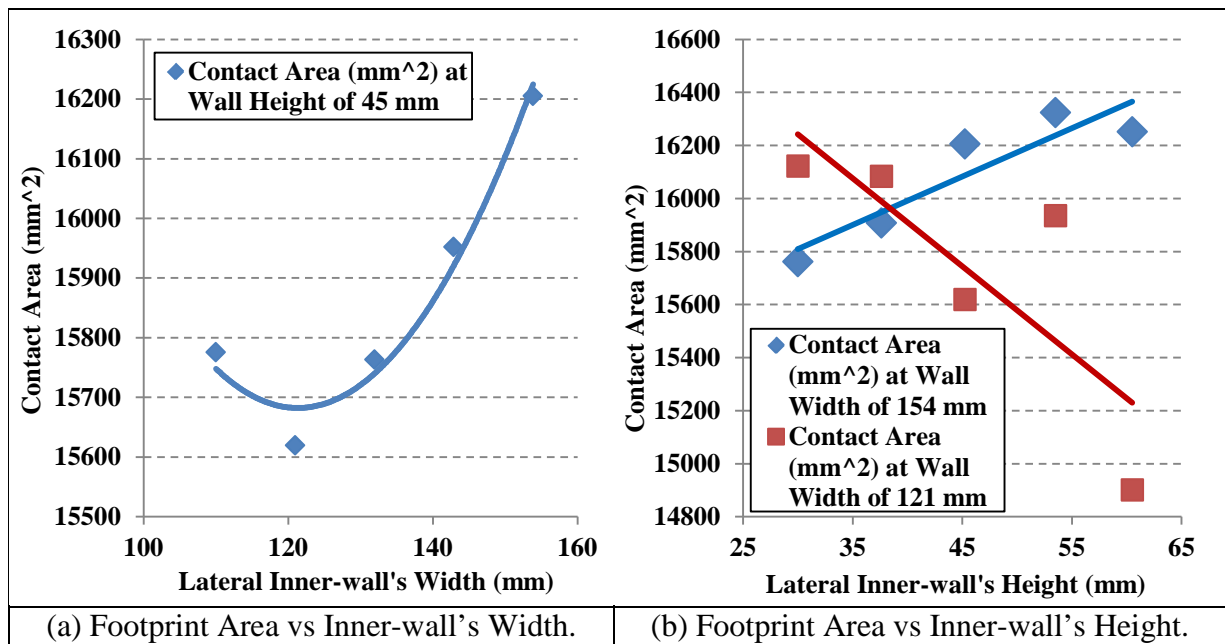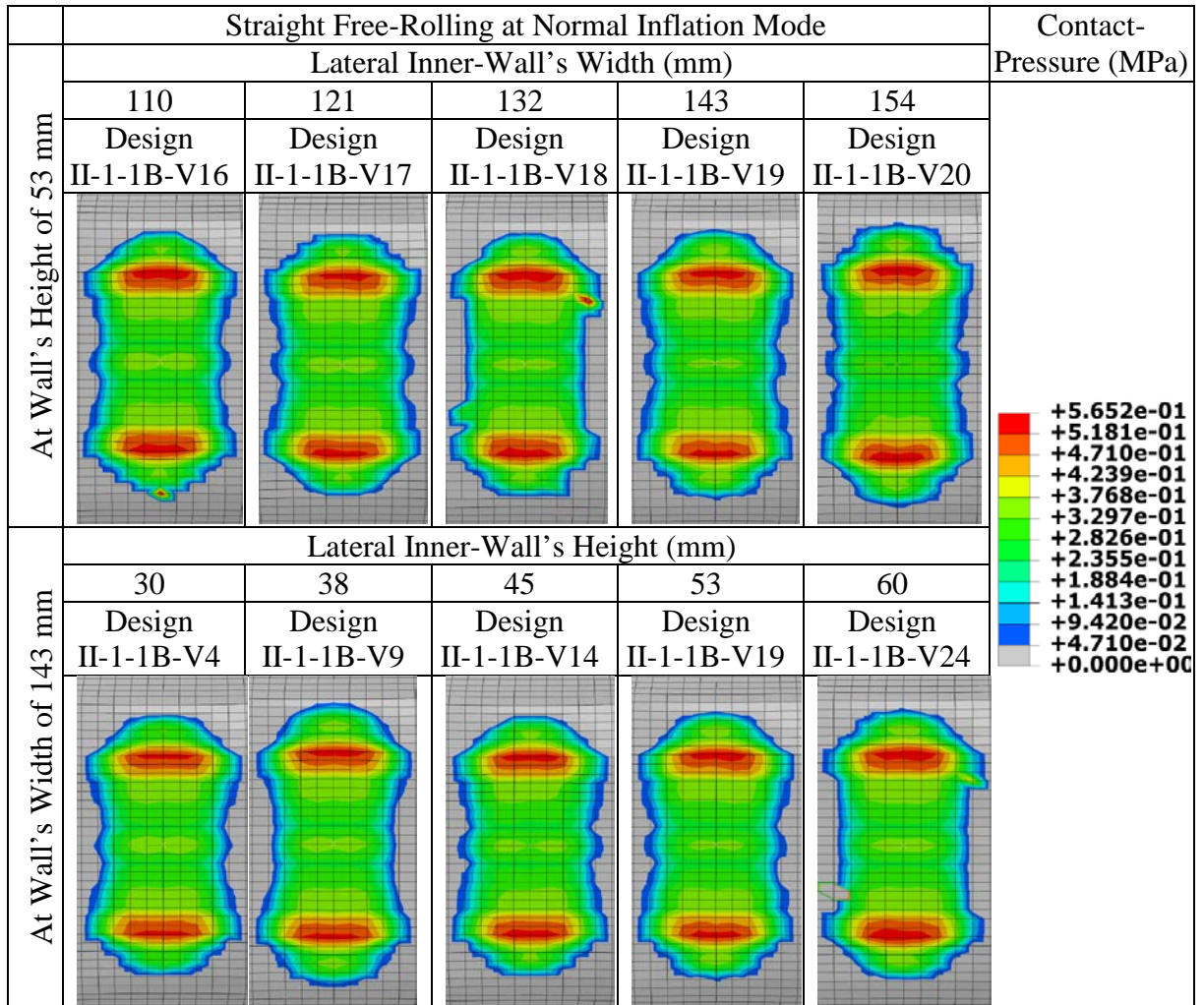Figure 5. Footprint Area versus Lateral Inner-Wall's Dimensions for Straight Free-Rolling.

However, increasing the lateral wall's height had adverse impact on footprint area at any fixed width equal to or below 132 mm. Besides being further away from the direct-loading path, such dimensional settings would make zone 2's volume and its side inner-walls smaller and stiffer that would require lesser deformational work to support the

tyre's tread under vertical loading according to the kinetic theory of gases and Hooke's law for spring-like objects. This is in line with the findings of Aldhufairi et al.[4].

In Table 3, the decrease of the lateral inner-wall's width was found to build-up more pressure at the footprint centre. This is as a narrower lateral inner-wall would bring the orientation of the cavity volumes in zones 1 and 2 more toward the tread centre leading to more pressure-displacement work at the centre during loading. On the other hand, increasing the lateral inner-wall's height would enhance the maximum pressure regions at the footprint shoulders. The enhancement is due to the reduction in both zone 2's volume and the height of its springy-like side inner-walls which makes the loading transferal via inner-walls to the tread shoulders region more rigid and direct. Such an aspect has contributed to boosting the tyre's radial stiffness with the increase of the lateral inner-wall's height as seen in Figure 6(a) for example. The lateral inner-wall's width had no impact on the radial stiffness.

Table 3. Contact-Pressure Pattern vs Lateral Inner-Wall's Dimensions.

	Straight Free-Rolling at Normal Inflation Mode					Contact-Pressure (MPa)
	Lateral Inner-Wall's Width (mm)					
At Wall's Height of 53 mm	110	121	132	143	154	
	Design II-1-1B-V16	Design II-1-1B-V17	Design II-1-1B-V18	Design II-1-1B-V19	Design II-1-1B-V20	
	Lateral Inner-Wall's Height (mm)					
At Wall's Width of 143 mm	30	38	45	53	60	
	Design II-1-1B-V4	Design II-1-1B-V9	Design II-1-1B-V14	Design II-1-1B-V19	Design II-1-1B-V24	

Contact-Pressure (MPa) scale:
+5.652e-01
+5.181e-01
+4.710e-01
+4.239e-01
+3.768e-01
+3.297e-01
+2.826e-01
+2.355e-01
+1.884e-01
+1.413e-01
+9.420e-02
+4.710e-02
+0.000e+00

(a) Radial Stiffness vs Inner-wall's Height.
(b) Rolling-Resistance vs Inner-wall's Height.
(c) Non-Uniformity vs Inner-wall's Height.
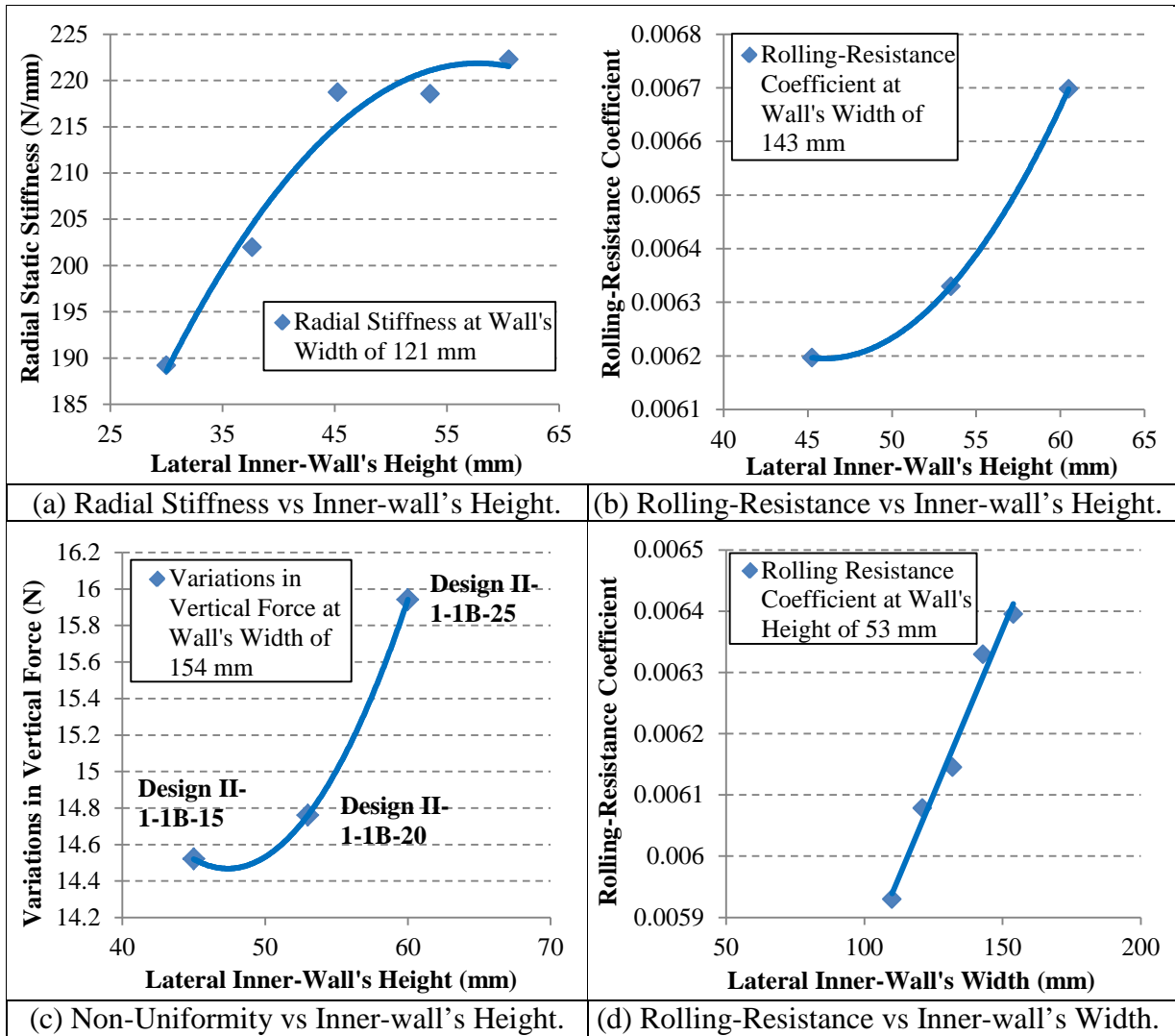(d) Rolling-Resistance vs Inner-wall's Width.

Figure 6. Effect of Lateral Inner-Wall Dimensions on Various Driving Requirements for Straight Free-Rolling.

Despite the added stiffness, a marginal increase in the rolling-resistance was observed as the lateral inner-wall's height was raised from 45 up to 60 mm as in Figure 6(b) for example. To find out the reason behind this, in Figure 6(c), the tyre's radial non-uniformity (i.e. vertical force variations at wheel-spindle), due to the difference in the tyre's inner-chambers design assuming negligible tyre manufacturing imperfections, was assessed similar to Aldhufairi et al.[4]. A slight increase in the tyre's radial non-uniformity

was found as the lateral inner-wall's height increased. This meant slightly higher continuous circumferential flexing of the tyre's tread during rolling was incurred with height increase. As the height increases, this would make zone 2's volume and its spring-like side inner-walls smaller, less resilient, easily disrupted, and unable to maintain tread profile in position more efficiently against the periodic circumferential oscillations induced by peristaltic-pumping effect during rolling. Nevertheless, II-1-1B's designs had lower radial non-uniformity than that of the standard design (i.e. 21.8 N).

At any fixed lateral inner-wall height above 30 mm, the rolling-resistance was observed to increase with the inner-wall's width increase as indicated in Figure 6(d). This is because a greater width would cause higher footprint deformation since the side inner-walls are moved closer to the direct vertical loading path.

Out of the twenty-five different volume designs, the best three designs in terms of tyre's grip were picked and further evaluated for the most balanced design for all driving requirements respectively. The three designs are "II-1-1B-15", "II-1-1B-20" and "II-1-1B-25".

In Figure 7, design "II-1-1B-20" was found to be the best choice for meeting all the driving requirements satisfactorily. For tyre's grip, "II-1-1B-20" has similar footprint area and contact-pressure to that of the standard design unlike the other designs. As for cornering, both "II-1-1B-20" and "II-1-1B-25" show improved cornering capabilities over the standard design whereas "II-1-1B-15" shows a close performance. In "II-1-1B-

20" and "II-1-1B-25", the curvy side inner-walls of zone 2 provides an enhanced lateral stability to the tyre through offering the tyre's sidewalls with an added cornering stiffness to counteract the related opposing vehicle centrifugal force(s). Also, under the direct support of the nearly un-deformed zone 1, zone 2 with its flexible side inner-walls provides a firm hold-down of the tyre's tread against the road for added grounding and to maintain better contact.

(a) Footprint Area at Straight Rolling (mm^2).

(b) Cornering Stiffness (N/deg).

(c) Footprint Area (mm^2) at 3 Degrees Slip.

(d) Rolling-Resistance Coefficient.

(e) Radial Static Stiffness (N/mm).

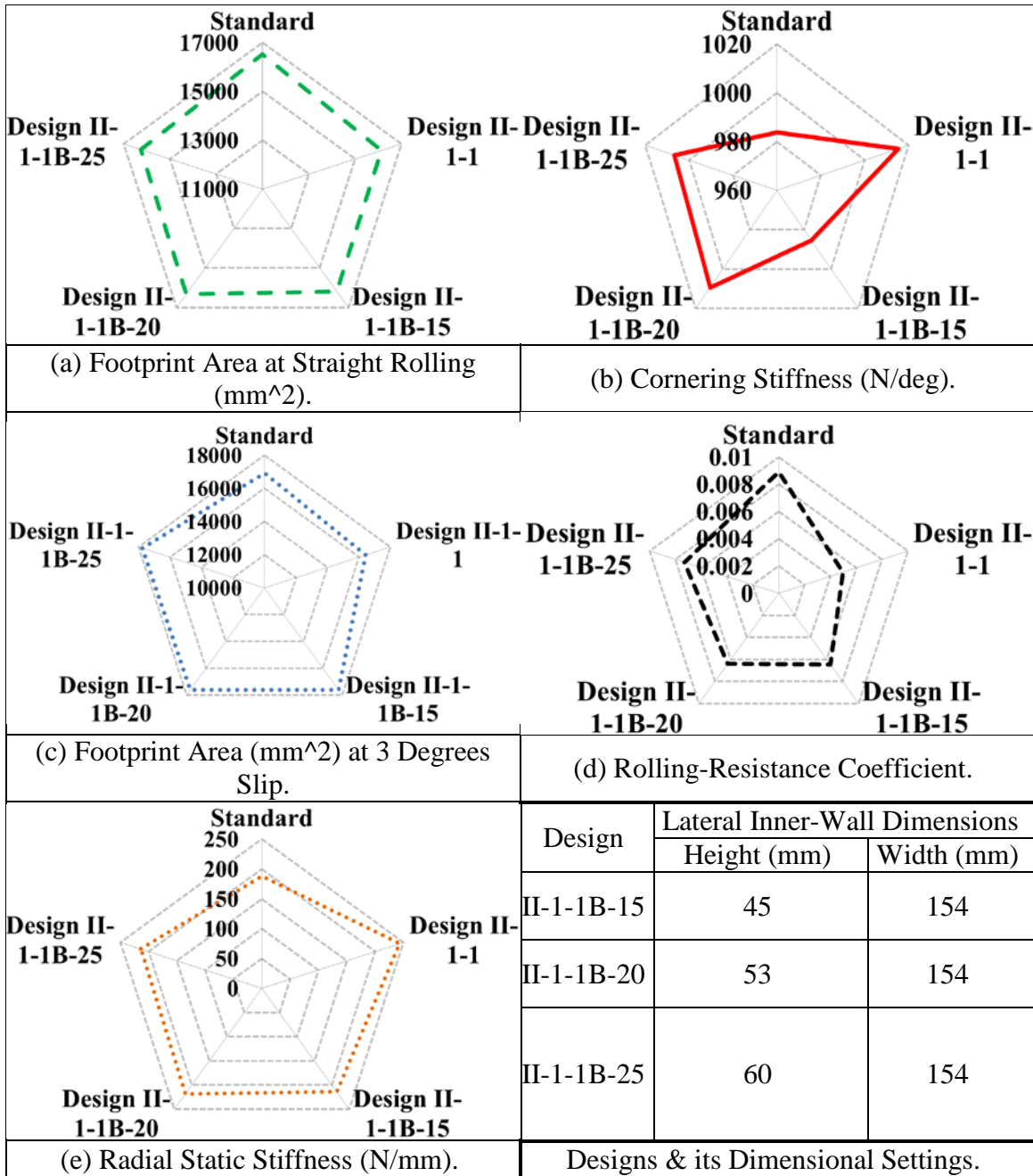| Design	Lateral Inner-Wall Dimensions	
	Height (mm)	Width (mm)
II-1-1B-15	45	154
II-1-1B-20	53	154
II-1-1B-25	60	154

Designs & its Dimensional Settings.

Figure 7. II-1-1B's Designs Performance at Normal Inflation Mode.

All three designs show lower roll-resistance than the standard design with "II-1-1B-15" and "II-1-1B-20" being nearly the same and the lowest. For the tyre's cushioning, all three designs exhibit higher radial stiffness with "II-1-1B-20" being slightly higher than

the other designs. Regardless, II-1-1B-20's stiffness is still within the acceptable limits, which is around 200-220 N/mm, for passenger-car tyres.[4, 28, 29]

3.3 Inflation Pressure Effect

Design "II-1-1B-20" was further evaluated for the effect of different inflation pressures on the overall performance and if a more optimum design is possible. The investigation involved changing the inflation pressure of the (L) and (R) side zones together with the same pressure to maintain a balanced run but independently from zone 2. The inflation levels within which those zones were inflated are shown in Table 4. The inflation levels were set close to that of the normal inflation mode (i.e. 220 KPa) in attempt to maintain the tyre's physical properties within safe and proper limits. Zone 1's inflation remained unchanged to maintain design stability. Using Full-Factorial DoE, nine different pressure settings were created and evaluated for the II-1-1B-20 design using Abaqus/Explicit.

Table 4. DoE's Factors and their Levels for Inflation Pressure Effect.

No	Factor	Pressure Levels (KPa)
1	Zone (2)	200
		220
		240
2	Side Zones (L) and (R)	200
		220
		240

Agreeing with Aldhufairi et al.[4], modifications to the zone 2's pressure have an apparent influence over the tyre's physical properties, whereas the side zones (L) and (R) have no obvious effect. Being in direct support of the tyre's tread, increasing zone 2's pressure leads to strengthening contact-pressure at tread shoulders and increasing the tyre's radial

stiffness causing a reduction in the footprint area (at straight rolling and cornering) along with the rolling-resistance in the process as seen in Figure 8. However, for cornering stiffness, zone 2's pressure has no apparent impact.

(a) Zone 2 Pressure vs Radial Stiffness.

(b) Zone 2 Pressure vs Footprint Area.

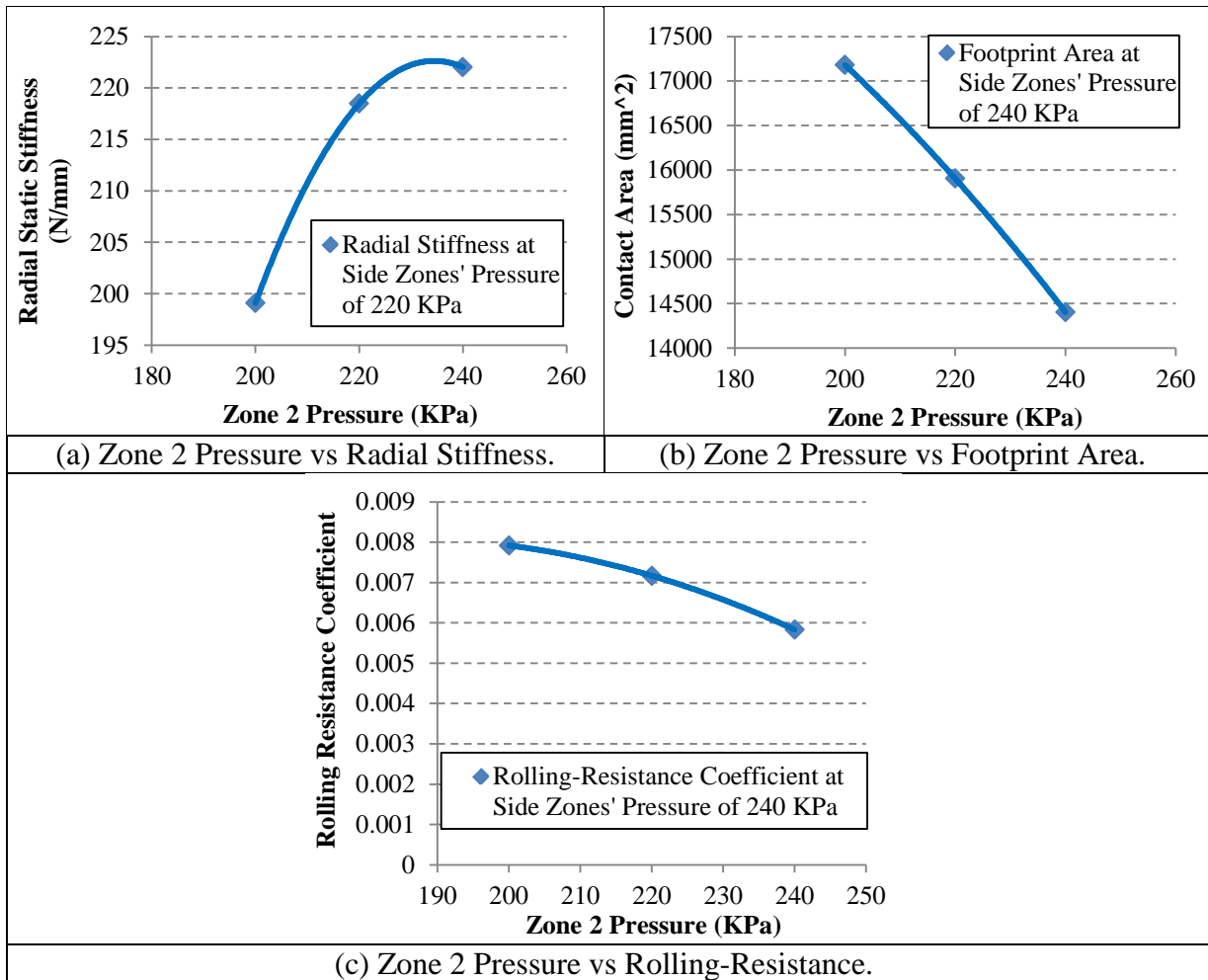(c) Zone 2 Pressure vs Rolling-Resistance.

Figure 8. Influence of Zone (2)'s Pressure on (a) Radial Stiffness, (b) Footprint Area, and

(c) Rolling-Resistance Coefficient (RRC) for Straight Free-Rolling.

Any pressure changes whether in zone 2 or side zones (L and R) were found to affect how the tyre responds to the different driving requirements with trade-offs involved usually as in Figure 9 for example. In that regard, "II-1-1B-20" design inflated at the

normal mode is concluded to still be the best choice to address the driving requirements

as it is tailored and optimised specifically at that mode for the different driving needs.

Design	Pressure Settings (KPa)		
	Zone 1	Zone 2	Zones (L & R)
Standard (220 KPa)	N/A	N/A	N/A
II-1-1B-20-3	320	200	240
II-1-1B-20-6	320	220	240
II-1-1B-20	320	220	220
II-1-1B-20-9	320	240	240

(a) Straight Rolling Footprint Area (mm^2). (b) Cornering Stiffness (N/deg). (c) Footprint Area (mm^2) at 3 Degrees Slip. (d) Rolling-Resistance Coefficient. (e) Radial Static Stiffness (N/mm). Designs & its Pressure Settings.
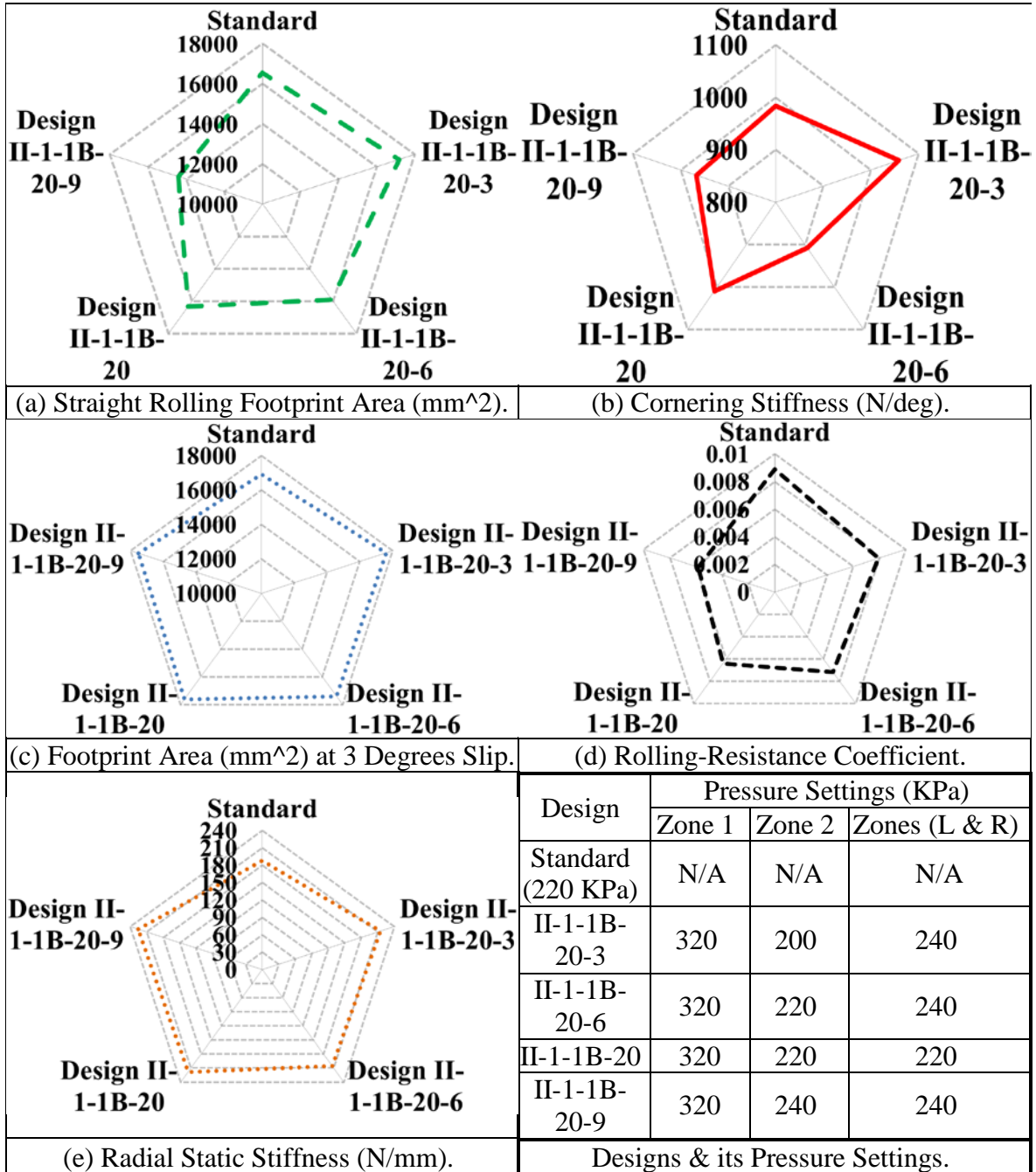
Figure 9. Samples of II-1-1B-20's Designs with different Pressures and its Performances.

Nevertheless, if the pressure is dynamically controlled, zone 2's pressure can be changed temporarily when needed to provide the tyre with extended versatility and enhanced performance to better address the driving condition at hand. At straight rolling on flat roads with marginal acceleration or braking, zone 2's pressure can be set at a higher level for reduced rolling-resistance and hence better fuel economy as is the case with the economy inflation mode of the "II-1-1B-20" design in Figure 10. At the economy mode, only zone 2 of the "II-1-1B-20" design can be further inflated to the highest pressure possible (i.e. 280 KPa) as per the design constraints in section (2.2) while keeping the other zones' pressure at the same level as in the normal mode.
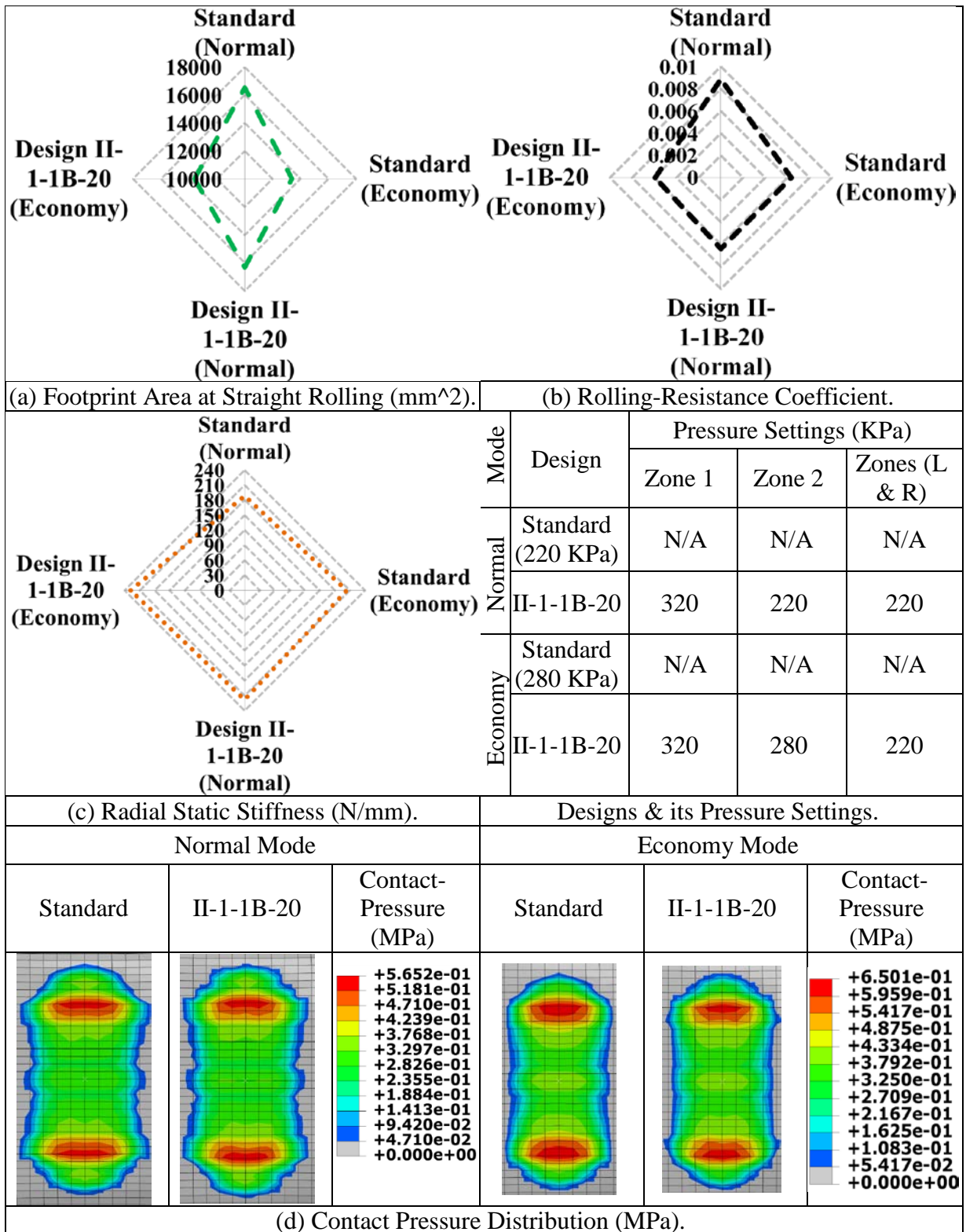
(a) Footprint Area at Straight Rolling (mm^2).

(b) Rolling-Resistance Coefficient.

(c) Radial Static Stiffness (N/mm).

Designs & its Pressure Settings.

Mode	Design	Pressure Settings (KPa)		
		Zone 1	Zone 2	Zones (L & R)
Normal	Standard (220 KPa)	N/A	N/A	N/A
	II-1-1B-20	320	220	220
Economy	Standard (280 KPa)	N/A	N/A	N/A
	II-1-1B-20	320	280	220

Normal Mode			Economy Mode		
Standard	II-1-1B-20	Contact-Pressure (MPa)	Standard	II-1-1B-20	Contact-Pressure (MPa)

(d) Contact Pressure Distribution (MPa).

Figure 10. Performances of "II-1-1B-20" Design and "Standard" Design at Normal and

Economy Modes for Straight Free-Rolling.

As indicated, the economy mode gives the "II-1-1B-20" design an added radial stiffness to further reduce rolling-resistance and improve fuel economy limited for usage in conditions like steady-state rolling on flat roads with minimum traction, braking and turning involved due to the tyre's grip and cushioning being undermined at that mode. However, if the driving conditions are to be changed in which the tyre's grip or cushioning is needed, the "II-1-1B-20" design is to be inflated back to the normal mode by just deflating zone 2's pressure from 280 KPa back to 220 KPa. Such driving conditions could be traction, braking, cornering or driving over bumpy roads.

The "II-1-1B-20" design in the economy mode gave a further rolling-resistance reduction of 7% compared to its normal mode and hence 35% to the normal mode of the standard design.

4. Conclusion

Design "II-1-1B-20" was found to be the best balanced "design-for-all" solution in which it met the targeted tyre grip, provided an improved cornering performance, and offered an acceptable cushioning level while lowering the rolling-resistance by ~28% compared to the standard design at the normal inflation mode as seen in Figure 10. The core design feature of the solution was the confinement of cavity-air into compact spaces in the direct vertical loading path to the tyre's tread, especially zone 2, which made the tyre's tread more independent from the side zones (L) and (R). Based on that, it was possible to maintain the tyre's contact-patch area while having an added radial stiffness.

The "design-for-all" solution (i.e. II-1-1B-20) had fewer chambers, where zone 2 was constructed with curvy spring-like side inner-walls, that allowed zone 2's structure to have greater elastic (stored) potential energy than the "II-1" design solutions. This has added more non-linear complexity to the tyre's structure and behaviour in which inconsistent cavity-volumetric effects on the driving requirements were found. However, it was noticeable that the rolling-resistance would slightly increase if zone 2's volume got smaller and/or if zone 2's side inner-walls were to lay-up closer to the direct vertical loading route.

"II-1-1B-20" design has the potential to provide extended versatility and more improved fuel economy if the inflation pressure is to be dynamically controlled during rolling. This is by changing zone 2's pressure only between 220 KPa (i.e. normal mode), for the necessary tyre's grip and cushioning, and 280 KPa (i.e. economy mode) for added radial stiffness and lower rolling-resistance according to the requirements of the driving/road conditions at hand.

In the economy mode, the "II-1-1B-20" design can provide a further rolling-resistance reduction of 7% in compared to its normal mode.

5. Future Work

To further optimise the current solution(s) for practical applications, the investigation scope is to be expanded to include assessing the solution's manufacturability, inflation

mechanisms, further operating factors, like rotational-inertia and temperature, and wider driving conditions like traction and braking.

On the solution's manufacturability, concepts of the potential manufacturing methods for future consideration are highlighted briefly below in Figures 11 and 12. For inflation mechanism, the "II-1-1B-20" design is to have its different cavities inflated through a network of flexible air channels connecting each chamber at its nearest point to a valve stem on the wheel rim. The "II-1-1B-20" solution can have either a single inflation mode (i.e. normal mode) to manually inflate and to use all time or an interchangeable mode (i.e. between normal and economy) depending on the driving condition which can be controlled through an auto-inflation system like Goodyear AMT or Aperia's Halo.
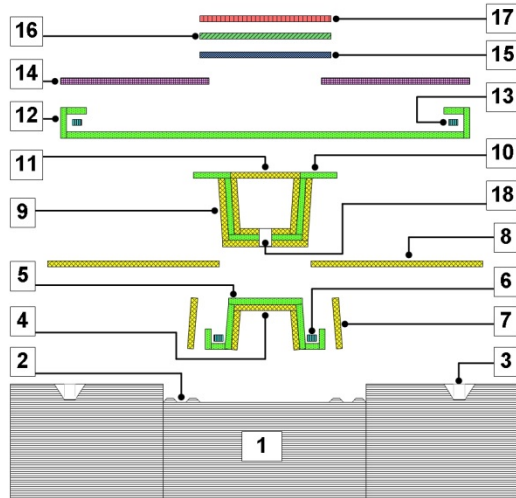
**Exploded Cross-sectional View of Tyre Structural Layers on Tyre Building Drum**

1 Dynamic & Triple Tyre Building Drum(s).

2 & 3 Grooves for Beads Mounting.

7 , 8 & 9 Airtight Inner Liners for Side Zones.

6 & 13 Steel Beads.

4 Airtight Inner Liner for Zone (1).

5 , 10 & 12 Body Plies.

11 Airtight Inner Liner for Zone (2).

4 to 7 Inner chamber (Zone (1)).

9 to 11 Inner chamber (Zone (2)).

14 Sidewalls.

15 Steel Belts.

16 Cap Plies.

17 Tread.

18 Inflation Hole.

Note:

- The different tyre structural layers are possible to produce using the conventional "extrusion" & "calendering" processes.

- Procedures (A) to (F) are similar to that of the conventional building process where a bonding film is added between the relevant layers when necessary to tie them.

- After building phase, the tyre is cured to fuse the different tyre layers into one solid structure & give the tyre its physical properties.
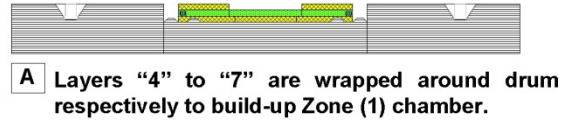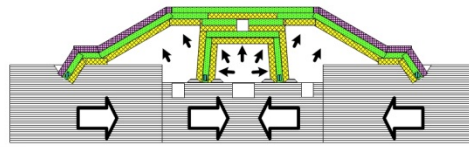
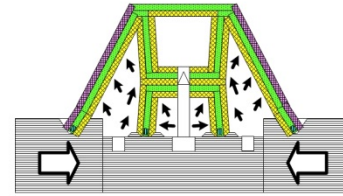A Layers "4" to "7" are wrapped around drum respectively to build-up Zone (1) chamber.
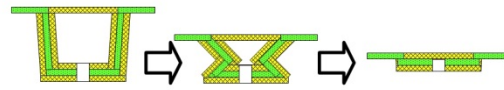
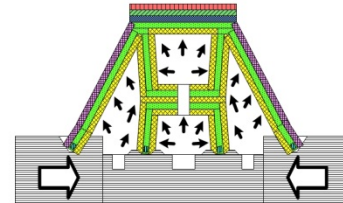B Zone (2) chamber is built-up independently from layers "9" to "11" then folded into thin flat layer.
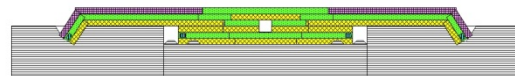
C Layers "8", followed by zone (2) chamber & then layers "12" to "14" are wrapped around drum respectively.

D Zone (1) chamber is inflated, drums move inward & side zones are inflated partially.

E Side zones are fully inflated and a puncture is made in zone (1) for inflation to pop-up zone (2).

F Zone (2) is fully inflated and layers "15", "16" & "17" are wrapped around drum respectively.

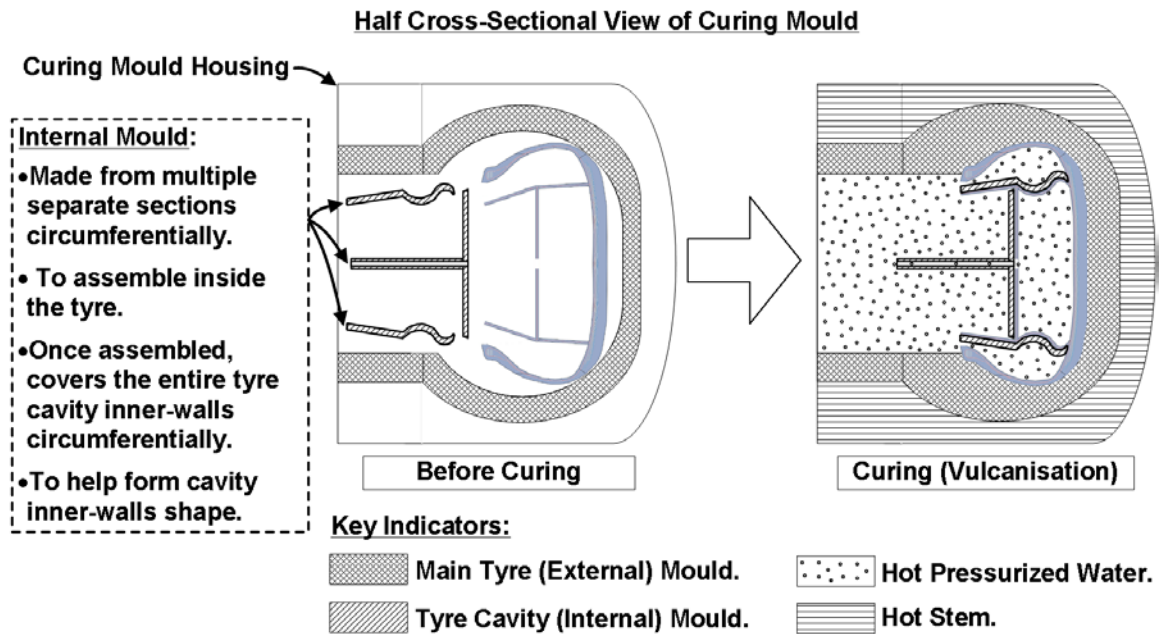Figure 11. On-Drum Building Procedure for "II-1-1B-20" Design.

32

Figure 12. Vulcanisation (Curing) Procedure for "II-1-1B-20" Design.

Declaration of Conflict of Interest:

Funding:

References

1.   Aldhufairi HS and Olatunbosun OA. Developments in tyre design for lower rolling resistance: a state of the art review. *Proceedings of the Institution of Mechanical Engineers, Part D: Journal of Automobile Engineering* 2017. DOI: https://doi.org/10.1177/0954407017727195.

2.   Shaw D. Interview: New force rising: Hee-Jong Lee, Nexen: The tech center chief on Nexen's European expansion. *Tire Technology International* 2015; 11: 30-34.

3.   Heeps G. Expo interview: Dufournier: A new tire labeling and R&D test facility. *Tire Technology International* 2015; 11: 36-38.

4.   Aldhufairi HS, Essa K and Olatunbosun O. Multi-chamber Tire Concept for Low Rolling-Resistance. *SAE International Journal of Passenger Cars - Mechanical Systems* 2019; 12. DOI: https://doi.org/10.4271/06-12-02-0009.

5.   Howard FA. *Safety pneumatic tire*. Patent US2969824A, 1961.

6.   Kenneth K and Brook O. *Multi-chamber safety tire*. Patent US20030131918A1, 2003.

7.   Mazhar MS. *Multi-chamber pressurizable tube for a tire*. Patent US6076580A, 2000.

8.   Seyed K. *Tire*. Patent US2525752A, 1950.

9.   Huber VR. *Tire*. Patent US3487870A, 1970.

10.   Cupp HN. *Automobile tire*. Patent US1989402A, 1935.

11.   Mclean WD. *Supplemental Shoe for Automobile Tires*. Patent US2735471A, 1956.

12.   Mcleod NW. *Multi-chambered vehicle tire*. Patent US2780266A, 1957.

13.   Lambe DM. *Dual-chamber pneumatic tire*. Patent US4293017A, 1981.

14.   Francesco M, Maria M and Marina M. *Tire for vehicles, composed of two concentric annular chambers*. Patent US2925845A, 1960.

15.   Bridgestone. Multi-chamber tyre extends thinking on stability. *European Automotive Design* 2006; 10: 12. SciTech Premium Collection.

16.   Evans R. Concept Tires: Future Proofs. *Tire Technology International* 2015; 3.

17.   Coyote. Coyote Boltless Beadlock System, https://www.coyoteents.com/beadlocks/ (2014).

18.   Hall G. *Pneumatic Tyre with Multiple Chambers*. Patent WO2014057282A1, 2014.

19.   Kubba AIS. *Intelligent tyre technologies*. University of Birmingham, Birmingham, UK, 2018.

20.   Aldhufairi HS and Essa K. Tire Rolling-Resistance Computation based on Material Viscoelasticity Representation. *Advances in Automotive Engineering* 2019; 1: 167-183. DOI: https://doi.org/10.12989/aae.2019.1.2.167.

21.   Yang X. *Finite element analysis and experimental investigation of tyre characteristics for developing strain-based intelligent tyre system*. PhD, University of Birmingham, Birmingham, UK, 2011.

22.   Kim T-W, Kim H-H, Jeong H-Y, et al. Determination of Prony Series Parameters and Rolling Resistance Simulation of a Tire. In: Yao Z, Yuan M and Zhong W, (eds.). *Sixth World Congress on Computational Mechanics in conjunction with the Second Asian-Pacific Congress on Computational Mechanics*. Beijing, China: Tsinghua University Press & Springer, 2004.

23.   Ghosh P, Saha A and Mukhopadhyay R. Prediction of tyre rolling resistance using FEA. *Constitutive Models for Rubber* 2003: 141-146.

24.   Mawby WD and Sauls J. *Improvement of tire uniformity through identification of process effects using singlet tire regression analysis*. Patent WO2012002949A1, 2012.

25.   Ask T. *Engineering for Industrial Designers and Inventors: Fundamentals for Designers of Wonderful Things*. " O'Reilly Media, Inc.", 2016.

26.   Myers R. *The basics of chemistry*. London, UK: Greenwood Publishing Group, 2003.

27.   Ji T. Concepts for designing stiffer structures. *The Structural Engineer* 2003; 81: 36-42.

28.   KuliKowsKi K and Szpica D. Determination of directional stiffnesses of vehicles' tires under a static load operation. *Eksploatacja i Niezawodność* 2014; 16: 66-72.

29.   Lee C-R, Kim J-W, Hallquist JO, et al. *Validation of a FEA tire model for vehicle dynamic analysis and full vehicle real time proving ground simulations*. Report no. 0148-7191, 1997. SAE Technical Paper.